

# TetraPackNet: Four-Corner-Based Object Detection in Logistics Use-Cases

1<sup>st</sup> Laura Dörr, 2<sup>nd</sup> Felix Brandt, 3<sup>rd</sup> Alexander Naumann, 4<sup>th</sup> Martin Pouls

Information Process Engineering  
FZI Research Center for Information Technology  
Karlsruhe, Germany  
doerr@fzi.de

**Abstract**—While common image object detection tasks focus on bounding boxes or segmentation masks as object representations, we propose a novel method, named TetraPackNet, using four-corner based object representations. TetraPackNet is inspired by and based on CornerNet and uses similar base algorithms and ideas. It is designated for applications where the high-accuracy detection of regularly shaped objects is crucial, which is the case in the logistics use-case of packaging structure recognition. We evaluate our model on our specific real-world dataset for this use-case. Baselined against a previous solution, consisting of a Mask R-CNN model and suitable post-processing steps, TetraPackNet achieves superior results (6% higher in accuracy) in the application of four-corner based transport unit side detection.

**Index Terms**—Convolutional Neural Networks, Deep Learning, Object Detection, Instance Segmentation, Logistics

## I. INTRODUCTION

While common image recognition tasks like object detection, semantic segmentation or instance segmentation are frequently investigated in literature, some applications could greatly benefit from more specialized technological approaches. In this work, we investigate how such specialized algorithm and neural network designs can improve the performance of visual recognition systems. For this purpose, we consider the use-case of logistics packaging structure recognition.



Fig. 1. Illustration of the use-case of packaging structure recognition.

The use-case of logistics packaging structure recognition aims at inferring the number, type and arrangement of standardized load carriers in uniform logistics transport units from a single image of that unit. It is illustrated in Fig. 1. In an approach to design a robust solution to this task, we identified the recognition of two visible transport unit side faces, by finding the exact positions of their four corner points, as

a reasonable sub-task [2]. Notably, our objects of interest, transport unit side faces, are of rectangular in real world. As the perspective projection is the main component of the imaging transformation, we can assume, that transport unit side faces can be accurately segmented by four image pixel coordinates in regular images of logistics transport units. Such assumptions are also valid in various other logistics use-cases such as package detection or transport label detection. The same holds for non-logistics applications like license plate or document recognition and other cases where objects of regular geometric shapes need to be segmented accurately to perform further downstream processing steps, often like image rectifications or perspective transforms.

To solve the challenge of detecting an object by finding a previously known number of feature points (e.g. four corner points) different approaches are possible. For instance, the application of standard instance segmentation methods and adequately designed postprocessing algorithms simplifying the obtained pixel masks, may be a viable solution. In this work, we aim to incorporate the geometrical apriori knowledge into a deep-learning based image recognition method by designing a convolutional neural network (CNN) detecting objects by four arbitrary corner points rather than regular bounding boxes. To achieve that, we build upon existing work by Law et al. [7], [8], enhancing the ideas of CornerNet. Fig. 2 illustrates the difference between commonly used object location representations, i.e. bounding boxes, and our four-corner based representation. The example image is taken from our use-case specific dataset. The objects indicated are two transport unit faces which need to be precisely localized for the motivating task of packaging structure recognition.



Fig. 2. Sample annotations. Left: Bounding box annotation. Right: Four-corner based annotation.

In this paper, we present a redesigned version of CornerNet,

namely TetraPackNet, which segments objects by four arbitrary corner points (i.e. tetragons) instead of bounding boxes or pixel-masks. We evaluate the approach on data concerning the use-case of logistics packaging structure recognition. Baselined against our previous solution to the sub-task of transport unit side corner detection, we show that TetraPackNet achieves improved detection rates. Further, we observe that predictions made by TetraPackNet are in general very accurate and corner positions are predicted precisely. For the use-case of logistics packaging structure detection, TetraPackNet represents a novel, very convenient method yielding improved detection results.

The rest of the paper is organized as follows: We summarize related work in Section II. The method and theoretical background’s are explained in Section III. Section IV concerns the example application of logistics packaging structure recognition and the corresponding dataset. We evaluate our approach in Section V. Finally, Section VI concludes our work with a summary and outlook.

## II. RELATED WORK

The primary use-case pushing our work is the one of logistics packaging structure detection, which we introduced in [2]. Apart from our own work, we are not aware of any other publications considering the same use-case.

As the number and frequency of publications focusing on image object detection is enormous, we refer to dedicated survey papers on the topic as introductory material. For instance, Wu et al. [15] or Liu et al. [11] give comprehensive overviews.

Our work builds on CornerNet [7], a recent work by Law et al., which aims to perform object detection without incorporating anchor boxes or other object position priors. Instead, corner positions of relevant objects’ bounding boxes are predicted using convolutional feature maps as corner heat maps. Corners of identical objects are grouped based on predicted object embeddings. This approach, which outperformed all previous one-stage object detection methods on COCO [10], was further developed and improved by Duan et al. [4] and Zhou et al. [16]. The follow-up work by Law et al. [8], CornerNet-Lite, introduced faster and even more accurate variations of the original CornerNet method. These advancements of the original CornerNet are not in our scope, we build upon the original work [7].

Another approach relevant for this work, is the deep learning based cuboid detection by Dwibedi et al. [5]. In this work in the context of 3D-reconstruction, cuboid shaped, class agnostic objects are detected and their vertices are precisely localized. We refrain from comparing to this work for several reasons, one of which is the requirement for richer image annotations (cuboid based, eight vertices per object). Further, we do not aim to reconstruct 3D-models from our images but aim to classify and interpret intra-cuboid information.

## III. METHOD

We present a novel method for four-corner based object detection based on CornerNet [7], a recent work of Law et

al. Whereas in traditional object detections, object locations are referenced by bounding boxes (i.e. top left and bottom right corner position), we work with more detailed locations described by four corner points. The resulting shapes are not limited to rectangles but comprise arbitrary tetragons, i.e. four-cornered polygons.

We use model, groundtruth and loss function designs very similar to those proposed in CornerNet [7]. All of these components, and our modifications for TetraPackNet, targeting tetragon-based object detection, are explained in the following sections. Fig. 3 gives an overview over our architecture. The additional components compared to CornerNet are highlighted.

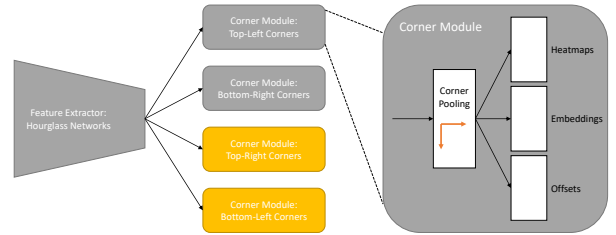


Fig. 3. TetraPackNet architecture. Differences to CornerNet are highlighted.

### A. Backbone Network

As suggested and applied by Law et al. [8], we use an hourglass network [13], namely Hourglass-54, consisting of 3 hourglass modules and 54 layers, as backbone network. Hourglass networks are fully convolutional neural networks. They are shaped like hourglasses in that regard, that input images are downsampled throughout the first set of convolutional and max pooling layers. Subsequently, they are upsampled to the original resolution in a similar manner. Skip layers are used to help conserve detailed image features, which may be lost by the network’s convolutional downsampling.

In TetraPackNet’s network design, two instances of the hourglass network are stacked atop each other to improve result quality.

### B. Corner Detection and Corner Modules

Following the backbone network’s hourglass modules, so-called corner modules are applied to predict precise object corner positions. CornerNet utilizes two such corner modules to detect top-left and bottom-right corners of objects’ bounding boxes. Our architecture includes four corner detection modules for the four corner types top-left, top-right, bottom-left and bottom-right. We do not detect corners of bounding boxes but precise corner locations of tetragon-shaped objects.

Analogously to the original CornerNet approach, each corner module is fully convolutional and consists of specific corner pooling layers as well as a set of output feature maps of identical dimensions. These outputs are corner heat maps, offset maps and embedding. They each work in parallel on identical input information: the corner-pooled convolutional feature maps.

We shortly revisit CornerNet’s specific pooling strategy. It is based on the idea that important object features can be found, when starting at a bounding box top left corner and moving in horizontal right or vertical bottom direction. More precisely, by this search strategy, object boundaries will be hit by bounding box definition. In CornerNet, max pooling is performed in the corresponding two directions for both bounding box corner types. The pooling outputs are added to one another and the results are used as input for corner prediction components. The authors show the benefits of this approach in several detailed evaluations. In our case, where precise object corners are instead of bounding box corners, one may argue that pooling strategies should be reconsidered. Still, for our first experiments, we retain this pooling approach.

The corner module’s three output sets are explained in the following. For each distinguished corner type, i.e. top left, top right, bottom left and bottom right corners in our case, the model includes one heat map predicting positions where the probability for a corner of the respective type is high. As the resolution of the corner module’s feature maps is lower than that of the original input image, additional location offsets are predicted for each potential corner candidate. To enable the assembly of four corresponding object corners to an object, embeddings are predicted for each corner. These embeddings aim to take such values that corners of the same object are as similar as possible, while those of corners of distinct objects differ significantly. The before-mentioned components corner pooling, corner heat map, offsets and embedding maps are combined to form a single corner prediction module.

More precisely, each corner module is a set of fully convolutional layers including corner heat maps for each object category, two offset maps for horizontal and vertical offset and, in case of one-dimensional embeddings, one embedding map. Moreover, we extended the CornerNet architecture to include four corner prediction modules instead of two. Additionally, TetraPackNet’s corner prediction modules do not aim to detect bounding box corners, but vertices of tetragonal-shaped objects.

### C. Ground-truth

Required image annotations are object positions described by the object’s four corner points, i.e. top left, top right, bottom left, bottom right corner. It is required that both right corners are further right as their counterparts and, equivalently, both top corners are further up as the corresponding bottom corners. For each groundtruth object one single positive location is added to each of the four ground-truth heatmaps. To allow for minor deviations of corner detections from these real corner locations, the ground-truth heatmaps’ values are set to positive values in a small region around every corner location. As proposed by CornerNet, we use a Gaussian function centered at the true corner position to determine ground-truth heatmap values in the vicinity of that corner.

In fig. 4 ground-truth heatmaps and detected heatmaps and embeddings are illustrated. The top row shows, cross-faded on the original input image, the ground-truth heatmaps

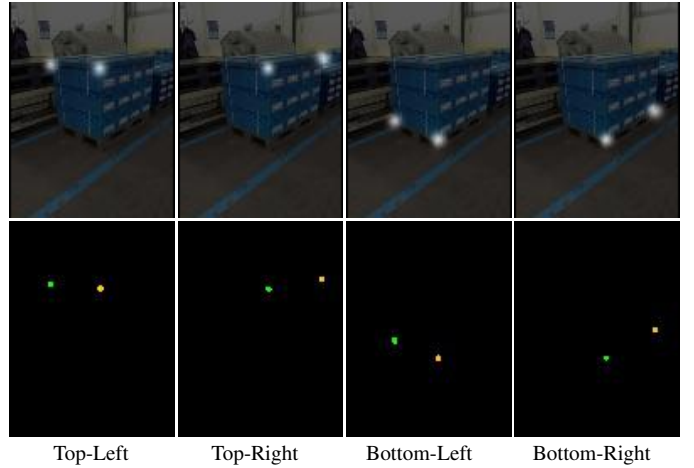


Fig. 4. Example heatmaps. Top row: Groundtruth. Bottom row: Detected heats and color-encoded embeddings.

for the four different corner types. There are two Gaussian circles in each corner type heatmap as there are two annotated ground-truth objects, i.e. two transport unit sides, in the image. The bottom row shows TetraPackNet’s detected heatmaps (for object type transport unit side) and embeddings in a single visualization: Black regions indicate positions where the predicted heat is smaller than 0.1. Wherever the detected heat value exceeds this threshold, the color indicates the predicted embedding value. To map embedding values to colors, the range of all embeddings for this instance was normalized to the interval from 0 to 1. Afterward Open CV’s Rainbow colormap was applied [1].

### D. Loss Function

The loss function used in training of our TetraPackNet model consists of several components:

$$L = L_{det} + w_{off} \cdot L_{off} + (w_{pull} \cdot L_{pull} + w_{push} \cdot L_{push}) \quad (1)$$

In our experiments, the loss component weights were set to  $w_{pull} = w_{push} = 0.1$  and  $w_{off} = 1.0$ , as proposed by Law et al. The individual loss components are explained in the following.

1) *Focal Loss  $L_{det}$* : The loss term’s first component  $L_{det}$  is a focal loss [9] variant, as proposed by CornerNet. This term aims to optimize heatmap corner detections by penalizing high heatmap values at points where there is no ground-truth corner location. Analogously, low heat values at ground-truth positive locations are penalized. Let  $y_{cij}$  be the ground-truth heat value for class  $c$  at location  $i, j$ . As mentioned in Section III-C ground-truth heat values are not binary, but positive-valued regions are drawn around each ground-truth corner location. To incorporate this in the focal loss formulation, an additional factor  $(1 - y_{cij})$  is added at locations where  $y_{cij} < 1$ . The focal loss for class  $c$  at location  $i, j$  is

$$L_{det}(c, i, j) = \begin{cases} (1 - h_{cij})^\alpha \log(h_{cij}) & y_{cij} = 1 \\ (1 - y_{cij})^\beta (h_{cij})^\alpha \log(1 - h_{cij}) & \text{otherwise} \end{cases} \quad (2)$$

where  $h_{cij}$  is the predicted heat value for class  $c$  at position  $i, j$ . The hyperparameters  $\alpha$  and  $\beta$  are set to  $\alpha = 2, \beta = 4$ . Overall, the focal loss is computed as

$$L_{\text{det}} = \frac{1}{N} \sum_{c=1}^C \sum_{i=1}^H \sum_{j=1}^W L_{\text{det}}(c, i, j) \quad (3)$$

where  $C$  is the overall number of classes and  $H \times W$  is the model’s heat map resolution.

2) *Offset Loss  $L_{\text{off}}$* : The offset loss  $L_{\text{off}}$  is used to penalize deviations in offset predictions in vertical and horizontal direction. As proposed in CornerNet, a simple smooth L1 Loss, comparing predicted and actual precise corner positions, is used.

3) *Pull and Push Loss  $L_{\text{pull}}$  and  $L_{\text{push}}$* : The last loss components, pull and push loss, are used to optimize the embedding values predicted at each potential corner location. As mentioned before, the objective is to predict embedding values as similar as possible for groups of corners of the same object instance. At the same time, embedding values of distinct object’s corners should be as far apart as possible. To achieve the first part of this objective, embedding similarity for corners of identical objects, the pull-loss  $L_{\text{pull}}$  is used. The pull loss is computed as

$$L_{\text{pull}} = \frac{1}{N} \sum_{k=1}^N \sum_{i \in \{tl, tr, bl, br\}} (e_i(k_i) - e(k))^2 \quad (4)$$

where  $k = 1, \dots, N$  enumerates the ground-truth objects and  $i = tl, tr, bl, br$  indicate the four corner types top left, top right, bottom left, bottom right. The position of corner  $i$  of ground-truth object  $k$  is denoted by  $k_i$ . Further,  $e_i$  denotes the embedding map for corner type  $i$  and therefore  $e_i(k_i)$  is the embedding value for corner  $i$  of ground-truth object  $k$ . The average value of the embedding values of all four corners of a ground-truth object  $k$  is given by  $e(k) = \frac{1}{4} \sum_{i \in \{tl, tr, bl, br\}} e_i(k_i)$ .

The push loss penalizes average embeddings of different objects being similar to each other, thereby “pushing” the embeddings of corners of different objects apart.

$$L_{\text{push}} = \frac{1}{N(N-1)} \sum_{k=1}^N \sum_{\substack{j=1 \\ j \neq k}}^N \max\{0, 1 - |e(k) - e(j)|\} \quad (5)$$

### E. Assembling Corner Detections to Objects

Once corner positions and their embeddings are predicted, these predictions need to be aggregated to form tetragon object detections. Compared to the CornerNet setup, this task appears more complex as each object is composed of four corners instead of only two. However, the original grouping implementation is based on Associative Embeddings [12], which is suitable for multiple data points in general, i.e. more than two. The same approach can be applied in our case.

To obtain an overall ranking for all detected and grouped objects, the four corner detection scores as well as the similarity of their embeddings, i.e. the corresponding pull loss

values, are considered. This final score for a detection  $p$  of class  $c$  consisting of four corners  $p_{tl}, p_{tr}, p_{bl}, p_{br}$  is computed as

$$\frac{1}{4} \sum_{i \in \{tl, tr, bl, br\}} h_i(c, p_i) + (e_i(p_i) - e(p))^2 \quad (6)$$

with  $e(p)$  being the average embedding for a set of four corners as before. Further,  $h_i(c, p_i)$  denotes the predicted heat value for class  $c$  and corner type  $i \in \{tl, tr, bl, br\}$  at position  $p_i$ .

Additionally, we only allow corners to be grouped which comply with the condition, that right corners are further right in the image than their left counterparts. Analogously bottom corners are required to be further down in the image than corresponding top corners.

### F. Implementation

Our implementation of TetraPackNet is based on the open source CornerNet Lite implementation by the Princeton Vision & Learning Lab [14]. This Python implementation is based on PyTorch 1.0 and uses standard COCO evaluation packages (pycocotools). To apply the above-mentioned modifications to the original method, several components were added or re-implemented. These changes include ground-truth data handling and data sampling, CNN redesign, loss function, output decode function, and evaluation preparations.

## IV. USE CASE AND DATA

### A. Logistics Unit Detection and Packaging Structure Analysis

Our work was developed in context of the logistics task of automated packaging structure recognition. The aim of logistics packaging structure recognition is to infer the number and arrangement of a well standardized logistics transport unit by analyzing a single RGB image of that unit. Fig. 1 illustrates this use-case. To infer a transport unit’s packaging structure from an image, the target unit, the unit’s two visible faces and the faces of all contained load carriers are detected using learning-based detection models. Several restrictions and assumptions regarding materials, packaging order and imaging are incorporated to assure feasibility of the task:

- All materials like load carriers and base pallets are known
- Transport units must be uniformly and regularly packed
- Images show two faces of each transport unit
- Transport units are fully shown in an upright orientation

The use-case and its setting, as well as limitations and assumptions are thoroughly explained in [2] and [3].

We designed a multi-step image processing pipeline to solve the task of logistics packaging structure recognition. The process’ individual steps can be summarized as follows:

- 1) Transport unit detection
- 2) Transport unit side and package unit face segmentation
- 3) Transport unit side analysis
- 4) Information consolidation

In step 1), whole transport units are localized within the image and input images are cropped correspondingly. (see Fig.

5 (a)) As a result, the input for step 2) is an image crop showing exactly one transport unit to be analyzed. Subsequently, transport unit sides (and package units) are detected precisely. This is illustrated in Fig. 5 (b). Step 3) aims to analyze both transport unit sides within the image. This involves a rectification of the image’s transport unit side region, in such a way to reconstruct a frontal, image boundary aligned view of each transport unit side. To perform such a rectification, the precise locations of the side’s four corner points are required. Fig. 5 (c) shows the rectified image patch of one transport unit side and illustrates package pattern analysis. Each transport unit side is analyzed independently and its packaging pattern is determined. In a last step, the informations of both transport unit sides are consolidated. The pipeline’s overall results are the precise number and arrangement of packages for each transport unit within an image.

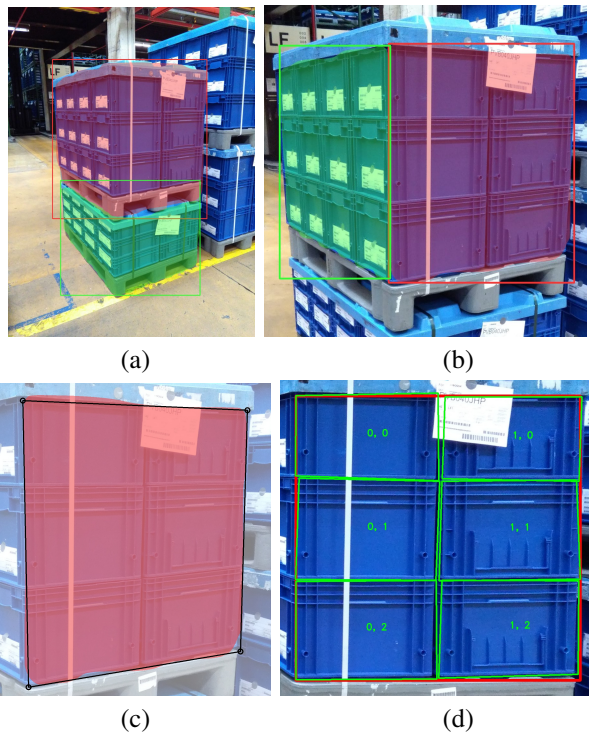


Fig. 5. Method Visualization. (a) Transport unit identification. (b) Transport unit side face segmentation. (c) Side detection post-processing: Approximation of segmentation mask by four corner points. (d) Rectified transport unit side.

In the context of this work, we focus on step 2) of our overall packaging structure recognition pipeline. Importantly, the simple detection and localization of these components represented by bounding boxes is not sufficient. As we aim to rectify transport unit face image patches in a succeeding step, the precise locations of the four corners of both transport unit faces are required. In our current solution to this task, a standard Mask R-CNN model [6] is used to segment the transport unit faces in the image. Afterwards, in a post-processing step, the segmentation masks, described by arbitrarily complex polygons, are simplified to consist of four points only. These points are refined by solving an optimization problem in such

a way that the tetragon described by these four points has the highest possible overlap with the originally detected object region. Fig. 5 (d) illustrates this four-corner approximation of segmentation masks.

In this work, we aim to simplify the previously described procedure. Instead of taking the detour via overly complex mask representations, we aim to utilize a tailored object detection method, namely TetraPackNet, which directly outputs the required four-corner based object representations.

### B. Specific Dataset

For training and evaluation of our TetraPackNet model, a custom use-case specific dataset of 1267 images was used. The dataset was acquired in a German industrial plant of the automotive sector. Each image shows one or multiple stacked transport units in a logistics setting. The rich annotations for each image also include four-corner based transport unit side annotations.

The dataset was split in three sub-sets: training, validation and test data. The test data set contains a handpicked selection of 163 images. For a set of images showing identical transport units it was ensured that either all or none of these images was added to the test data set. The remaining 1104 images were split into train and validation data randomly, using a train-validation ratio of 75-25.

## V. EXPERIMENTS

In this section, we examine the performance of TetraPackNet. First, TetraPackNet is trained on our use-case data and results are compared to a suitable baseline model. This evaluation is performed using standard and use-case specific metrics. In an additional section, we motivate and propose an alternative corner grouping strategy and evaluate the approach.

### A. Evaluations

1) *Transport Unit Side Detection*: To evaluate TetraPackNet for our use-case, we compare its performance on the use-case specific dataset described in Section IV-B with a standard Mask R-CNN model. Both models were trained for the single-class problem of transport unit side detection, as described in Section IV-A.

a) *Setup*: In both cases, the same dedicated training, validation and tests splits were used. Training and evaluation were performed on an Ubuntu 18.04 machine on a single GTX 1080 Ti GPU unit.

Two different training scenarios are evaluated for both models: First, the models are trained to localize transport unit sides within the full images. In a second scenario, the cropped images are used as input instead: as implemented in our packaging structure recognition pipeline (see Section IV-A), all images are cropped in such ways that each crop shows exactly one whole transport unit. For each original image, one or multiple such crops can be generated, depending on the number of transport units visible within the image. This second scenario is comparatively easier as exactly two transport unit sides are present in each image and the variance of the scales of transport units within the image is minimal.

TABLE I  
OBJECT DETECTION EVALUATION RESULTS FOR THE WHOLE IMAGE SCENARIO ON OUR 163-IMAGE TEST DATASET.

Model	AP	AP <sub>0.5</sub>	AP <sub>0.75</sub>	AP <sub>0.9</sub>
Mask R-CNN	67.5	91.7	84.5	13.4
TetraPackNet	80.0	83.6	82.5	82.5

TABLE II  
INSTANCE SEGMENTATION EVALUATION RESULTS FOR THE WHOLE IMAGE SCENARIO ON OUR 163-IMAGE TEST DATASET.

Model	AP	AP <sub>0.5</sub>	AP <sub>0.75</sub>	AP <sub>0.9</sub>
Mask R-CNN	58.7	87.0	66.5	16.5
TetraPackNet	75.5	83.6	83.5	66.7

TABLE III  
OBJECT DETECTION EVALUATION RESULTS FOR THE CROPPED IMAGE SCENARIO ON OUR 163-IMAGE TEST DATASET.

Model	AP	AP <sub>0.5</sub>	AP <sub>0.75</sub>	AP <sub>0.9</sub>
Mask R-CNN	82.9	99.0	97.9	50.2
TetraPackNet	94.6	96.0	96.0	96.0

TABLE IV  
INSTANCE SEGMENTATION EVALUATION RESULTS FOR THE CROPPED IMAGE SCENARIO ON OUR 163-IMAGE TEST DATASET.

Model	AP	AP <sub>0.5</sub>	AP <sub>0.75</sub>	AP <sub>0.9</sub>
Mask R-CNN	80.3	98.9	91.5	54.6
TetraPackNet	91.1	96.0	95.0	85.2

b) *Training Details:* In both trainings, we tried to find training configurations and hyperparameter assignments experimentally. However, due to the high complexity of CNN trainings and its time consumption, an exhaustive search for ideal configurations could not be performed. Most likely, improvements are possible in both cases. Still, we consider the results presented in the following an affirmation of our proposed architecture TetraPackNet.

To achieve fair preconditions for both training tasks, the following prerequisites were fixed. Both models were trained for the same amount of epochs: The training of the Mask R-CNN baseline model included 200.000 training steps using a batch size of 1, whereas the TetraPackNet training included 100.000 training steps with a batch size of 2. Input resolution for both models was limited to 512 pixels per dimension. Images are resized such that the larger dimension measures 512 pixels and aspect ratio is preserved. Subsequently, padding to quadratic shape is performed. In both trainings, we considered similar image augmentation methods: random flip, crop, color distortions and conversion to gray values. Of these options, only the ones yielding improved training results were retained.

c) *Standard Metric Results:* As standard evaluation metric, the COCO dataset’s [10] standards are used. We report average precision (AP) at intersection over union (IoU) threshold of 0.5 ( $AP_{0.5}$ ), 0.75 ( $AP_{0.75}$ ) and averaged for ten equidistant IoU thresholds from 0.5 to 0.95 ( $AP$ ). Tables I and II show the corresponding results for the object detection (bounding box based) as well as the instance segmentation (mask based) formulation of the problem.

Considering the values at the lowest IoU threshold examined (0.5), the baseline Mask R-CNN outperforms TetraPackNet by

significant margins. E.g. in the bounding box evaluation (table I), Mask R-CNN’s  $AP_{0.5}$ -value is 8.1 points higher than that of TetraPackNet (91.7 vs. 83.6). However, as the IoU threshold for detections to be considered correct increases, TetraPackNet gains the advantage. When regarding performance values at IoU threshold 0.75, Mask R-CNN, with an  $AP_{0.75}$  of 84.5, still provides a higher amount of detections with bounding boxes classified as correct. Still, when looking at the segmentation mask evaluation in table II instead, TetraPackNet achieves a significantly higher precision of 83.5, compared to 66.5 for Mask R-CNN. This observation can be expanded for the average precision scores at higher IoU thresholds: TetraPackNet begins to gain advantage over our baseline method as detection accuracy requirements increase. This is illustrated in fig. 6 (top), which visualizes the same segmentation mask evaluation results shown in table II.

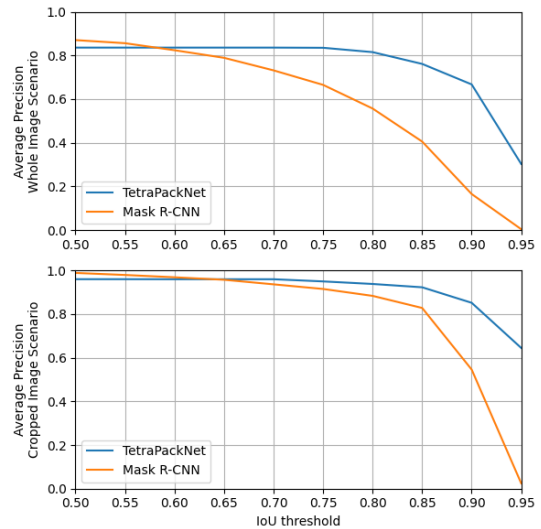


Fig. 6. Average precisions at different IoU thresholds for TetraPackNet and Mask R-CNN baseline model. Top: Whole image scenario. Bottom: Cropped image scenario.

Very similar observations can be made for the cropped image scenario: TetraPackNet clearly outperforms the reference model Mask R-CNN when high accuracies are required. The corresponding evaluation results are shown in tables III and IV, and in the bottom part of Fig. 6.

Overall, the results suggest that TetraPackNet does not detect quite as many ground-truth transport unit sides as our Mask R-CNN baseline model on a low accuracy basis. At the same time, the predictions made by TetraPackNet appear to be very precise as average precision steadily remains on a high level as IoU accuracy requirements are increased. For our use-case of packaging structure recognition, these are desirable conditions, as our processing pipeline requires very accurate transport unit side predictions.

d) *Use-Case Specific Results:* To investigate performance and benefits of TetraPackNet for our specific use-case, other metrics than standard COCO Average Precision are needed. Within our use-case of packaging structure detection,

TABLE V  
USE-CASE SPECIFIC EVALUATION RESULTS ON OUR 163-IMAGE TEST DATASET.

Model	Accuracy	Average IoU (Positives only)
Mask R-CNN & post-processing	86.6	0.908
TetraPackNet	95.7	0.958

the precise localization of each transport unit side’s four corner points is crucial. Therefore, we baseline our results against our previous approach, which relies on Mask R-CNN to obtain transport unit side segmentation masks. In a post-processing step, four corner points giving the best approximation of these masks were found by solving a suitable optimization task. Input to the task in our image processing pipeline, and for these evaluation, are cropped images showing exactly one full transport unit.

As evaluation criteria two different metrics are computed, both of which are based on the standard value of intersection over union (IoU). For each ground-truth transport unit side, the IoUs with its assigned detection, represented by four corner points, is computed. Thereby, only the two highest-ranked detections of each method are considered, as there are exactly two transport unit sides in each image. Detections are assigned from left to right, based on the a-priori knowledge, that one transport unit side is positioned clearly further left than the other one. Only for cases where less than one transport unit side was detected by the methods under consideration, an IoU-based assignment, with IoU threshold 0.5, is performed. If no detection was matched to a ground-truth object, the IoU value for this side is set to 0.

The first metric we compute is an overall accuracy value. Therefore, we assume a ground-truth transport unit side to be detected correctly if it has an IoU of at least 0.8 with its assigned detection. The accuracy of the transport unit side detection is equal to the percentage of ground-truth transport unit sides detected correctly.

The second evaluation value we compute, is the average IoU for correctly assigned detections. For the use-case at hand this is a reasonable and important assessment, as the succeeding packaging structure analysis steps rely on very accurate four-corner based transport unit side segmentations [2]. Table V shows the corresponding results.

Overall, this use-case specific evaluation requiring a high detection accuracy is dominated by our novel approach TetraPackNet. The latter achieves higher rates of high-accuracy transport unit side detections: TetraPackNet correctly detects 95.1% of transport unit sides, whereas the baseline method only achieves 86.6% in this metric. Additionally, if only considering sufficiently accurate detections of both models, the average IoU of the detections output by TetraPackNet was significantly higher (0.053 IoU points on average) than for those of our baseline method. We deduce the suitability of TetraPackNet for our application.

## B. Evaluation: Embedding-Free Detection to Object Grouping Method

The experiment of this section is motivated by an observation made by manual examination of TetraPackNet’s detection errors. In case of multiple packaging units in a single image, error often occurred in the corner to object assignments. It seems to be the case that embeddings are not a suitable predictor for corner assignments. Especially, for instance in case of stacked transport units, the embeddings of both left (or right) transport unit sides seem to be very similar for both transport units. This can be explained by the visual similarity often present for highly standardized transport units. A corresponding example is shown in fig. 7. In the left image, individual detection results are indicated by differently colored tetragons. The yellow, light blue and white tetragons represent examples with incorrectly assigned corners. The right image shows the color encoding of the bottom-right corner embeddings. Obviously, the embeddings for the left-most transport unit side are very similar for both top and bottom transport unit.



Fig. 7. False assignment of object corners to objects and color-encoded embedding values of bottom-right corners.

Thus, an additional strategy for the assembly of objects from corner detections was implemented. Contrary to the original grouping strategy, this alternative solution does not require prediction of any corner embedding values. Instead, we assume all instances of one object class to be non-overlapping and of similar sizes. For the use-case of packaging structure recognition and the detection of transport unit sides, or even package unit faces, this is a valid prerequisite. Given such preconditions, we try to find correct objects by preferring valid corner groupings of smaller sizes. Here, valid means the previously mentioned conditions, that right corners are further right, and bottom corners are further down within the image, holds true.

Formally, we proceed as follows: For each given valid set of four (refined) corner points  $p_{tl}, p_{tr}, p_{bl}, p_{br}$  of identical class  $c$  we compute the corresponding object extent  $E$ :

$$E(p_{tl}, p_{tr}, p_{bl}, p_{br}) = |p_{tr} - p_{tl}| + |p_{br} - p_{tr}| + |p_{bl} - p_{br}| + |p_{tl} - p_{bl}| \quad (7)$$

TABLE VI

INSTANCE SEGMENTATION EVALUATION RESULTS FOR DIFFERENT OBJECT GROUPING STRATEGIES ON OUR 163-IMAGE TEST DATASET.

Model	AP	AP <sub>0.5</sub>	AP <sub>0.75</sub>	AP <sub>0.9</sub>
Grouping by embeddings	75.5	83.6	83.5	66.7
Grouping ordered by extent	64.5	72.6	72.5	53.4

We compute a extent-sensitive object score as

$$\sum_{i \in \{tr, tl, br, bl\}} p(c, p_i) + (1 - \frac{E(p_{tl}, p_{tr}, p_{bl}, p_{br})}{2 \cdot (H + W)}) \quad (8)$$

where  $H \times W$  is the heatmap resolution as before.

We rank all possible corner groupings correspondingly. Objects are accepted in this order where it is ensured that each corner point is exploited only once. Precisely speaking, if an object grouping of four corners is accepted, all other possible groupings of lower score containing one identical corner detection are discarded.

The results for the scenario of transport unit side detection on complete images (without cropping) in terms of the COCO standard metrics are shown in table VI. Though the embedding-free approach does not perform quite as well as the one relying on embedding values (AP 64.5 vs. 75.5), the results are still acceptable. The average precision value of 64.5 is quite comparable to our baseline approach based on Mask R-CNN which scored 64.2 regarding identical metrics.

This is still work in progress and we have not concluded our experiments regarding embedding-free object groupings. At this point, we assume that improvements to the results above are possible and that a performance competitive to the previous embedding-based approach can be achieved.

## VI. SUMMARY AND OUTLOOK

### A. Results Summary

We presented TetraPackNet, a novel object detection model architecture tuned for, but not limited to, the task of logistics packaging structure recognition. The model is an adoption and extension of CornerNet detecting objects based on four independent corner points rather than two-corner based bounding boxes.

We trained and evaluated TetraPackNet on our own use-case specific dataset. For the dedicated task, the observed performance results in a higher accuracy (superior by 6 percentage points) compared to a previous approach involving a standard Mask R-CNN model and suitable post-processing.

### B. Future Work

The applicability of TetraPackNet to our use-case of logistics packaging structure recognition will be evaluated further. First of all, we plan to apply the model to package unit detection. This task is additionally challenging as, in general, a large number of densely arranged package faces of very similar appearance need to be detected. On the other hand, a-priori knowledge about the regular package arrangement might allow for specific corner detection interpretations and even

interpolations (e.g. in case of single missing corner detections). Additionally, we plan to extend TetraPackNet to specialized detection tasks including even more than four corner points. In our case of logistics transport unit detections, a lot of a-priori knowledge about object structure, shape and posture is given. This can be exploited by integrating specific transport unit templates into the detection model: one can define multiple additional characteristic points (e.g. base pallet or packaging lid corners) which are to be detected by a highly specialized deep learning model.

Further, we will investigate further ablation scenarios. As mentioned before, corner pooling strategies adopted from CornerNet might not be ideal for TetraPackNet and its applications. Thus, for instance, experiments with different corner pooling functions will be executed.

At the same time, as mentioned above, TetraPackNet is not limited to the use-case of packaging structure recognition or logistics in general. Other applications might include license plate or document detection. We plan to affirm our positive results by evaluating TetraPackNet on an additional dataset of a different use-case.

## REFERENCES

- [1] G. Bradski and A. Kaehler. *Learning OpenCV: Computer vision with the OpenCV library.* " O'Reilly Media, Inc.", 2008.
- [2] L. Dörr, F. Brandt, M. Pouls, and A. Naumann. Fully-automated packaging structure recognition in logistics environments. *arXiv preprint arXiv:2008.04620*, 2020.
- [3] L. Dörr, F. Brandt, M. Pouls, and A. Naumann. An image processing pipeline for automated packaging structure recognition. In *Forum Bildverarbeitung 2020*, page 239. KIT Scientific Publishing, 2020.
- [4] K. Duan, S. Bai, L. Xie, H. Qi, Q. Huang, and Q. Tian. Centernet: Keypoint triplets for object detection. In *Proceedings of the IEEE/CVF International Conference on Computer Vision*, pages 6569–6578, 2019.
- [5] D. Dwibedi, T. Malisiewicz, V. Badrinarayanan, and A. Rabinovich. Deep cuboid detection: Beyond 2d bounding boxes. *arXiv preprint arXiv:1611.10010*, 2016.
- [6] K. He, G. Gkioxari, P. Dollár, and R. Girshick. Mask r-cnn. In *Proceedings of the IEEE international conference on computer vision*, pages 2961–2969, 2017.
- [7] H. Law and J. Deng. Cornernet: Detecting objects as paired keypoints. In *Proceedings of the European Conference on Computer Vision (ECCV)*, September 2018.
- [8] H. Law, Y. Teng, O. Russakovsky, and J. Deng. Cornernet-lite: Efficient keypoint based object detection. *arXiv preprint arXiv:1904.08900*, 2019.
- [9] T.-Y. Lin, P. Goyal, R. Girshick, K. He, and P. Dollár. Focal loss for dense object detection. In *Proceedings of the IEEE international conference on computer vision*, pages 2980–2988, 2017.
- [10] T.-Y. Lin, M. Maire, S. Belongie, J. Hays, P. Perona, D. Ramanan, P. Dollár, and C. L. Zitnick. Microsoft coco: Common objects in context. In *European conference on computer vision*, pages 740–755. Springer, 2014.
- [11] L. Liu, W. Ouyang, X. Wang, P. Fieguth, J. Chen, X. Liu, and M. Pietikäinen. Deep learning for generic object detection: A survey. *International journal of computer vision*, 128(2):261–318, 2020.
- [12] A. Newell, Z. Huang, and J. Deng. Associative embedding: End-to-end learning for joint detection and grouping. *arXiv preprint arXiv:1611.05424*, 2016.
- [13] A. Newell, K. Yang, and J. Deng. Stacked hourglass networks for human pose estimation. In *European conference on computer vision*, pages 483–499. Springer, 2016.
- [14] Princeton Vision & Learning Lab. Cornernet-lite: Training, evaluation and testing code.
- [15] X. Wu, D. Sahoo, and S. C. Hoi. Recent advances in deep learning for object detection. *Neurocomputing*, 396:39–64, 2020.
- [16] X. Zhou, D. Wang, and P. Krähenbühl. Objects as points. *arXiv preprint arXiv:1904.07850*, 2019.